Published in final edited form as:
Inf Process Med Imaging. 2009 ; 21: 276–287.

Voxel-by-Voxel Functional Diffusion Mapping for Early Evaluation of Breast Cancer Treatment

Bing Ma[*,1], **Charles R. Meyer**[1], **Martin D. Pickles**[2], **Thomas L. Chenevert**[1], **Peyton H. Bland**[1], **Craig J. Galbán**[1], **Alnawaz Rehemtulla**[3], **Lindsay W. Turnbull**[2], and **Brian D. Ross**[1]
Bing Ma: bingm@umich.edu

[1]Department of Radiology, University of Michigan Medical School, Ann Arbor, MI, 48109, USA

[2]Centre for Magnetic Resonance Investigations, Division of Cancer, Postgraduate Medical School, University of Hull, HU3 2JZ Hull, UK

[3]Department of Radiation Oncology, University of Michigan Medical School, Ann Arbor, MI, 48109, USA

Abstract

Quantitative isotropic diffusion MRI and voxel-based analysis of the apparent diffusion coefficient (ADC) changes have been demonstrated to be able to accurately predict early response of brain tumors to therapy. The ADC value changes measured during pre- and post-therapy interval are closely correlated to treatment response. This work was demonstrated using a voxel-based analysis of ADC change during therapy in the brains of both rats and humans, following rigidly registering pre- and post-therapeutic ADC MRI exams. The primary goal of this paper is to extend this voxel-by-voxel analysis to assess therapeutic response in breast cancer. Nonlinear registration (with higher degrees of freedom) between the pre- and post-treatment exams is needed to ensure that the corresponding voxels actually contain similar cellular partial contributions due to soft tissue deformations in the breast and compartmental tumor changes during treatment as well. With limited data sets, we have observed the correlation between changes of ADC values and treatment response also exists in breast cancers. With diffusion scans acquired at three different timepoints (pre-treatment, early post-treatment and late post-treatment), we have also shown that ADC changes across responders within 5 weeks are a function of time interval after the initiation of treatment. Comparison of the experimental results with pathology shows that ADC changes can be used to evaluate early response of breast cancer treatment.

1 Introduction

Breast cancer patients may elect to receive neoadjuvant chemotherapy before surgery. If the patient elects to have surgery as soon as possible to remove the tumor following diagnosis, neoadjuvant chemotherapy may be performed while the patient waits for the surgery. For the patient who chooses to undergo a longer course of neoadjuvant chemotherapy before surgery, usually several complete treatment cycles will be conducted and the surgery will remove whatever tumor mass remains. A demonstrated benefit of such neoadjuvant chemotherapy for responders is the achievement of tumor shrinkage, allowing breast conservation surgery for a proportion of the patients. Unfortunately 20–25% of all breast cancer patients do not respond to chemotherapy. It would be beneficial to identify those patients who are not responding to

[*]This work is supported in part by NIH grants 1P01CA85878, 1P01CA87634, and P50CA93990.

Correspondence to: Bing Ma, bingm@umich.edu.

their neoadjuvant chemotherapy so that a change in treatment management may be introduced earlier, sparing patients from potentially ineffective and toxic treatment. Some existing methods of detecting response, e.g., clinical palpation or radiological RECIST measurements, typically support accurate detection of response only after 8 – 10 weeks of chemotherapy. Identifying surrogates that can predict therapeutic outcome earlier or more accurately than current methods would be valuable to tailor treatment to individual patients.

Large clinical trials assume that the degree of response of the primary tumor to neoadjuvant chemotherapy correlates with patient survival [1–4]. This suggests tumor response may be a surrogate for evaluating the effect of chemotherapy and could therefore be an important prognostic indicator of treatment outcome.

Imaging modalities can be used to track tumor changes resulting from response to a particular chemotherapy regimen. Several imaging modalities have been used in assessing the extent of response to primary breast cancer treatment. These modalities include mammography, ultrasound, and anatomical magnetic resonance imaging (MRI). Unfortunately, the sensitivity of these imaging technologies is inadequate in predicting pathological complete response (pCR) when compared to clinical examination [5].

Given that diffusion MRI is sensitive to structure at the cellular level, it has the potential to detect and quantify cellular changes that occur in response to successful therapeutic intervention [6]. It has been increasingly used to predict the magnitude of response of cancer to chemotherapy [6–9]. Diffusion MRI, combined with voxel-based analysis of the apparent diffusion coefficient (ADC) changes during treatment has been used to predict early response to cancer treatment. Researchers have demonstrated a fundamental correlation between ADC changes within the tumor measured over the pre- to early post-treatment interval and the response of various brain tumors to therapies [6–15]. This correlation has been shown both in primary and metastatic tumors of multiple organ systems in both rats and humans. In this paper we extend the voxel-by-voxel analysis to assess early response of breast cancer treatment and establish that the same correlation exists in breast cancer and can be used as an early biomarker of cell death and a potential surrogate for clinical outcome.

In previous work on tracking changes in ADC values over the pre- to early post-treatment interval for brain tumors, affine registration was performed on the interval exams. A functional diffusion map (fDM), i.e., a voxel-by-voxel scatter plot of the registered pre- vs. post-therapy ADC values, was then constructed assuming that the voxels in the registered pre- and post-treatment volumes contain approximately the same cells. FDM analysis has been shown to provide a strikingly accurate early biomarker for determining therapy response in the brain tumor patients. Affine registration works remarkably well in these brain tumors because the tumor's geometry changes during treatment are constrained and thus well modeled by rigid body deformation (rotation and translation) or at most include some shearing due to the high gradients used in diffusion echo planar imaging.

However, the scenario is completely different for breast tumors. The breast consists of soft, deformable tissue and thus nonlinear warping is definitely needed to accomplish accurate alignment of pre- and post-treatment volumes so that corresponding voxels in the registered pre- and post-treatment volumes contain similar cellular partial contributions. Automatic nonlinear registration algorithms are within reach with only modest effort if the breast in question is cropped down to the approximate boundaries of the lesion by the user, which is common practice in image processing.

2 Methods

2.1 Diffusion MRI for Assessing Cancer Treatment Response

Diffusion weighted MRI allows quantitative investigation of the changes in the Brownian motion of water [16]. Intracellular water is tightly bound and high density cellular packing in cancers has low diffusivity. During an effective treatment cancerous cells are killed and lyse increasing the ADC in the affected regions.

Each diffusion-weighted image series is comprised of 2 images per anatomic slice: b_0 ($b = 0$) which has relatively high signal-to-noise ratio (SNR) and no diffusion-weighting, and b_{high} (e.g., $b = 700$ or 800 s/mm^2) which has heavy diffusion weighting and lower SNR. The diffusion weighted imaging (DWI) is rotationally invariant, i.e., isotropic. That is, the diffusion weighted images are insensitive to the directionality of water mobility by combination of DWI along three orthogonal directions. ADC maps were calculated by simply taking the logarithm of the ratio of images acquired at two diffusion weightings and then scaling by the inverse of the difference in b-values (assuming low SNR pixels are properly eliminated):

$$ADC = \frac{1}{b_{high} - b_0} \log \frac{S_{b_0}}{S_{b_{high}}}, \tag{1}$$

where S_{b0} and $S_{b_{high}}$ are the signal intensities recorded at $b = 0$ and $b = b_{high}$ s/mm^2, respectively.

A functional diffusion map (fDM) is constructed from the registered pre- and post-treatment image volumes. It consists of a color overlay image of therapeutic-induced ADC change (post-treatment minus pre-treatment) within the tumor (Fig. 1, right column) and the scatter plot of corresponding pre- and post-treatment ADC values (Fig. 1, left column). The fDM provides the ability to objectively segment the tumor into three colored regions based on the magnitude and direction of ADC change. Red region includes voxels whose ADC values have increased significantly during treatment, represented by "V_i"; blue region includes voxels whose ADC values have decreased significantly, represented by "V_d"; and green region includes voxels whose ADC values have not changed significantly compared with the null hypothesis, represented by "V_0". The scatter plots (Fig. 1, left column) were found to correlate with subsequent tumor response.

The voxel-by-voxel fDM approach has a significant advantage over volumetric summary metrics (i.e., mean change in ADC values). Mean ADC change within the entire tumor during therapy can be an early response estimator, but it has its limitations. Therapeutic response is usually quite complex including often opposite and competing effects: some cells die causing increased extracellular water and associated increased ADC values while some other cells proliferate at a high rate leading to decreased extracellular water and ADC values. Averaging the ADC changes over the entire tumor cancels out some (if not most) of these opposite effects and thus makes mean ADC change insensitive to spatial heterogeneity of treatment response.

2.2 Nonlinear Image Registration

A prerequisite for proper fDM analysis using pre- and post-therapy breast examinations is that the corresponding pre- and post-treatment image voxels contain similar cellular partial volume contributions. Mutual information (MI) based image registration algorithms are employed to align the pre- and post-treatment scans.

Tumor volumes of interest (VOI) were drawn on the high resolution anatomical image volumes and were warped from the anatomical volumes onto the pre-treatment (pre-Tx) diffusion

volumes denoted as the reference; a warping registration is necessary due to the susceptibility artifacts in the diffusion, echo-planar acquisitions not present in the anatomical, spin echo acquisitions. Subsequent registrations between the pre- and post-treatment (post-Tx) diffusion scans are also warped to account for repositioning deformations to the breast as well as any compartmental changes to the tumor.

Warping is accomplished using thin plate splines where the degrees of freedom (DOF) of the warp is related to the local mutual information density and volume of the tumor. The user only picks the loci of 3 control points in the floating tumor volume that approximate their loci in the reference tumor volume. The multiscale registration first implements rigid body registration, then low DOF warping, and finally full DOF warping [17]. The details of registration are as follows:

1. Automatically generate a distance sorted set of hexagonal close-pack control points in the cropped reference volume based on the highest density of control points supported by the mutual information of the dataset pairs to be registered. Let N be the total number of control points in this pre-generated set and these control points are sorted according to decreasing pairwise distances.
2. Choose the first 3 control points from the pre-generated point set in the reference volume.
3. Provide 3 approximate homologous control points in the floating volume that correspond to the positions of the first 3 control points in the reference set, again based on the resultant cropping of the user.
4. Apply rigid body registration to roughly align the floating exam to the reference.
5. More points from the pre-generated control point set in the reference volume are chosen for warping registration where the number of points is set in the registration schedule. The corresponding control points in the floating exam are generated using the resultant geometric transformation from the previous registration schedule. Since the reference control points are distance sorted in order from most distant to nearest, iteratively increasing the number of points not only implements an increasing DOF warping, but also a decreasing scale space registration.
6. Repeat step 5 until all N control points have been used in the last schedule line which yields the final solution, subject to no folding. Folding is prevented by checking the sign of the Jacobian deformation after each optimization. If negative, the reference and corresponding homologous control point pair closest to the loci of the most negative Jacobian value are removed, and the optimization is repeated until no negative Jacobian values occur in the solution. This strategy allows the algorithm to locally decrease the DOF and control point density to follow local MI density variations.

2.3 Determination of Thresholds

After registration is accomplished, the voxel-by-voxel fDM analysis will be applied to estimate treatment response based on the changes in ADC values during treatment. A primary task in fDM analysis is to set appropriate thresholds which determine how much ADC change can be treated as significantly increased/decreased. Due to the complicated nature of noise distribution, analytical derivation of the thresholds is impossible. Instead, we utilize a small set of patient data as the training data to experimentally determine the appropriate thresholds to segment the tumor areas. These thresholds are then applied to the data acquired by the University of Hull MRI Centre for early evaluation of treatment response.

The training set comes from an ongoing double-blinded feasibility study at the University of Michigan investigating the role of diffusion MRI and functional diffusion maps as an early biomarker to predict therapeutic response for breast cancer. In the imaging protocol patients with breast cancer that have elected neoadjuvant chemotherapy prior to surgery receive 2 baseline exams (affectionately named "coffee-break" exams), typically within a 15 minute interval where the patient is removed from the scanner and then repositioned for the second scan; these short interval exams are used to observe the null change distribution since no macroscopic changes have occurred to the tumor in this interval. The initiation of the first cycle of chemotherapy (adriamyacin/cyclophosphamide) typically follows within one day of the short interval exams. In this acquisition the high b value is 800 s/mm^2. ADC maps are computed from the interleaved b_0 and b_{800} diffusion weighted MRI acquisitions by substituting b_{high} with b_{800} in Equation (1).

For each pair of registered ADC images a 128 × 128 joint density histogram (JDH) is constructed by incrementing the count of the 2D histogram defined by the two ADC values of the registered tumor (a demonstration is shown in Fig. 2(a)). Ideally the resulting JDH will be symmetric about the diagonal assuming no tumor growth/recession in such a short period. However, in practice for each experimental sample of the null distribution JDH is slightly biased. To remove this inevitable bias, the sum of the JDH and its transpose is used to derive the variance of the null change, now unbiased distribution. A 95% confidence interval is applied to the null hypothesis test: If a test value is outside the interval, the test rejects the null. With currently available 5 patients' pre-treatment coffee-break exams, the average 95% confidence interval for ADC changes is $[-0.5; 0.5]\times10^{-3}$mm^2/s rounded to one decimal place. Since the increased ADC values associated with cell death and increased diffusion in extracellular water are our primary interest in predicting therapy response, the 97.5th percentile threshold corresponding to an ADC change of 0.5×10^{-3} mm^2/s is the threshold we choose for evaluating the treatment response in the University of Hull data. In other words, if the ADC change of a voxel is larger than 0.5×10^{-3} mm^2/s, this voxel belongs to the region of significantly increased ADC values, i.e., V_i.

2.4 FDM Analysis on the University of Hull Data [18]

We evaluate the diffusion weighted MRI combined with functional diffusion mapping analysis as an imaging response biomarker using the clinical data provided by the University of Hull clinical trial [18]. Together 27 patients with biopsy-proven breast cancer were scanned prior to and after the first, second and fourth (final scheduled) cycle of neoadjuvant chemotherapy to allow monitoring tumor changes by using diffusion weighted MRI. Treatment cycles consisted of epirubicin (90 mg/m^2) and cyclophosphamide (600 mg/m^2) administered at 3 week intervals. Patients were scanned either on a 3.0 or 1.5T scanner (GE Healthcare, Milwaukee, WI, USA) in combination with dedicated bilateral breast coils. Different field strengths do not affect the study results as ADC values, in principle, are not dependant on B0 field strength.

Diffusion weighted MRI was acquired axially with a water-only excitation, singleshot, dual spin-echo EPI sequence with the following parameters: TR, 4000 ms, fractional TE, 74 ms (3.0 T) or 98 ms (1.5 T); FOV, 340 × 340 mm; matrix, 128 × 128; slice, 5 mm; gap, 1 mm; 10 averages; b values, 0 and 700 s/mm^2, applied in all three orthogonal directions. DWI scans were acquired in 2 min 40 s at both field strengths. A dual spinecho EPI sequence was utilized since this sequence reduces eddy currents and, therefore, image distortions with the addition of an extra refocusing pulse after the conventional refocusing pulse.

Not all 27 data sets were used to study the correlation between ADC changes and treatment response. Some diffusion scans only include partial tumor scans and are treated as inadequate for assessing the treatment efficacy and therefore excluded from this study. Eventually we have 14 complete data sets.

To test the capability of ADC changes in assessing early treatment response, the joint distribution histogram of registered pre-treatment and post-treatment ADC values was investigated. An example of JDH is shown in Fig. 2(b). This distribution represents the treatment effect distribution and clearly reveals that ADC values have increased in several ways: first the mean has moved upwards, and secondly there is a larger portion of voxels above the 97.5^{th} percentile line derived from the null distribution based on the training data sets. The corresponding scatter plot is shown in Fig. 3. Here red indicates the presence of voxels whose ADC changes (post-treatment minus pre-treatment) are greater than the 97.5^{th} percentile of the null distribution (i.e. regions of cell kill and limited noise, "V_i"); green indicates voxels whose changes are within the 2.5^{th} – 97.5^{th} percentiles (regions of no significant change, "V_0"); and blue indicates changes that are below the 2.5^{th} percentile of the null (regions of continued tumor growth and limited noise, "V_d"). The voxels in the "red" region (V_i) count for 12.25% of the entire tumor volume in Fig 2(b). Note that while 2.5% of these voxels are expected noise and distributed as spatially uncorrelated, single voxels, the treatment effect increment above 2.5% is typically seen as spatially correlated, i.e., connected voxels. We repeated this functional diffusion mapping analysis on each of the data set in this study and percentage_V_i (the percentage of the V_i volume over the entire tumor volume) was calculated. We subtracted 2.5% from percentage_V_i to remove the effect of the noise inherent in the null distribution so that percentage_V_i reflects the actual percentage of voxels with increased ADC values.

3 Experimental Results

The pathological outcome was used to remove 4 non-responding patients from the regression fit to the response of neoadjuvant therapy. The chemotherapeutic agent for the first two cycles of neoadjuvant therapy was exactly the same and consistent response was expected during this time period. The first post-therapy data acquisition took place within 2–12 days after the initiation of the first cycle of treatment. The second post-therapy data acquisition took place within 11–19 days after the initiation of the second cycle of treatment and within 32–39 days after the initiation of the first treatment cycle. Note that the post-treatment scans were acquired within different numbers of days after the initiation of therapy. To study the role of ADC changes between pre- and post-therapy examinations as an early indicator of treatment effectiveness, we focus on the relationship between ADC changes and time intervals after the initiation of treatment. In our study post-treatment scans include the diffusion scans obtained after both the first and the second cycle of treatment.

Percentage_V_i as a function of the number of days after treatment for responders is shown in Fig. 4. Responders are indicated by "×" while non-responders by "o". For most responder cases, their percentage_V_i is above zero, which means that there are voxels in the tumor whose ADC values have increased significantly during treatment.

To investigate the correlation of ADC changes and interval lengths after the initiation of treatment, linear regression was performed and the regression line (red line) with p-value 0.03 was shown in Fig. 4. We clearly observe that these five-week-post-treatment exams exhibit a larger effect size in ADC change compared to their one-week-post-treatment counterparts. After some duration we would expect the treatment effect on diffusion level to off or even drop back to the null effect after most cancer cells have been killed.

A blue line was drawn to connect the two time points for each patient. Please note that the post-first-treatment scans for cases 07 and 10 were obtained only 5 days after the initiation of treatment and it is highly likely that it is too soon to see any cellular change in the tumor. However, it was 33 days after the initiation of therapy that post-second-treatment exams were taken and the interval was long enough for the treatment to take effect. Therefore, these two

cases exhibit large increases in the ADC values in the post-second-treatment exams compared to their pre-treatment scans.

Logistic regression analysis was performed to further examine the correlation of ADC changes during treatment with clinical outcomes. A logistic regression fit with $p = 0.009$ at five weeks post-treatment demonstrated that the probability of a responsive treatment is strongly associated with increased ADC values. We observed 1 false positive and 1 false negative for a sensitivity of 90% and a specificity of 75%. On the other hand, logistic regression at one week post-treatment showed no capability of separating responders from non-responders.

4 Conclusion

We have extended voxel-by-voxel functional diffusion mapping analysis to assess early response to breast cancer treatment. The thresholds of significant ADC changes were derived from short interval exams and were used to evaluate treatment efficacy based on ADC changes during treatment. With limited data sets, experimental results have shown that ADC changes have the potential to be used to assess treatment effectiveness and are likely an increasing function of the temporal interval after the initiation of treatment within an as yet unknown time limit. Clearly the ratio of therapeutic effect size to noise at one week post-therapy is small; at 5 weeks post-therapy the opposite appears to be true. Logistic regression analysis has further revealed that ADC changes at five weeks post-therapy are highly correlated with treatment response.

References

1. Fisher B, Bryant J, Wolmark N, Mamounas E, Brown A, Fisher ER, Wickerham DL, Begovic M, DeCillis A, Robidoux A, Margolese RG Jr, ABC, Hoehn JL, Lees AW, Dimitrov NV, Bear HD. Effect of preoperative chemotherapy on the outcome of women with operable breast cancer. Journal of Clinical Oncology 1998;6:2672–2685. [PubMed: 9704717]
2. Kuerer HM, Newman LA, Smith TL, Ames FC, Hunt KK, Dhinga K, Theriault RL, Singh G, Binkley SM, Sneige N, Buchholz TA, Ross MI, McNeese MD, Buzdar AU, Hortobagyi GN, Singletary SE. Clinical course of breast cancer patients with complete pathologic primary tumor and axillary lymph node response to doxorubicin-based neoadjuvant chemotherapy. Journal of Clinical Oncology 1999;17:460–469. [PubMed: 10080586]
3. Bonadonna G, Valagussa P, Brambilla C, Ferrari L, Moliterni A, Terenziani M, Zambetti M. Primary chemotherapy in operable breast cancer: eight-year experience at the Milan cancer institute. Journal of Clinical Oncology 1998;16:93–100. [PubMed: 9440728]
4. Buchholz TA, Hill BS, Tucker SL, Frye DK, Kuerer HM, Buzdar AU, McNeese MD, Singletary SE, Ueno NT, Pusztai L, Valero V, Hortobagyi GN. Factors predictive of outcome in patients with breast cancer refractory to neoadjuvant chemotherapy. Cancer J 2001;7:413–420. [PubMed: 11693900]
5. Schott AF, Roubidoux MA, Helvie MA, Hayes DF, Kleer CG, Newman L, Pierce LJ, Griffith KA, Murray S, Hunt KA, Paramagul C, Baker LH. Clinical and radiologic assessments to predict breast cancer pathologic complete response to neoadjuvant chemotherapy. Breast Cancer Res Treat 2005;92:231–238. [PubMed: 16155794]
6. Chenevert TL, Stegman LD, Taylor JMG, Robertson PL, Greenberg HS, Rehemtulla A, Ross BD. Diffusion magnetic resonance imaging: an early surrogate marker of therapeutic efficacy in brain tumors. J Natl Cancer Inst 2000;92(24):2029–2036. [PubMed: 11121466]
7. Moffat BA, Chenevert TL, Lawrence TS, Meyer CR, Johnson TD, Dong Q, Tsien C, Mukherji S, Quint D, Gebarski SS, Robertson PL, Junck LR, Rehemtulla A, Ross BD. Functional diffusion map: a noninvasive MRI biomarker for early stratification of clinical brain tumor response. Proc Natl Acad Sci USA 2005;102(15):5524–5529. [PubMed: 15805192]
8. Ross BD, Moffat BA, Lawrence T, Mukherji S, Gebarski S, Quint D, Johnson TD, Junck L, Robertson P, Muraszko K, Dong Q, Meyer CR, Bland P, McConville P, Geng H, Rehemtulla A, Chenevert TL.

Evaluation of cancer therapy using diffusion magnetic resonance imaging. Mol Cancer Therapy 2003;2:581–587.

9. Hamstra DJ, Chenevert TL, Moffat BA, Johnson TD, Meyer CR, Mukherji S, Quint DJ, Gebarski SS, Xiaoying F, Tsiena C, Lawrence TS, Junck LR, Rehemtulla A, Ross BD. Evaluation of the functional diffusion map as an early biomarker of time-to-progression and overall survival in high grade glioma. Proc Natl Acad Sci USA 2005;102(46):16759–16764. [PubMed: 16267128]
10. Chenevert TL, Meyer CR, Moffat BA, Rehemtulla A, Mukherji SK, Gebarski SS, Quint DJ, Robertson PL, Lawrence TS, Junck L, Taylor JM, Johnson TD, Dong Q, Muraszko KM, Brunberg JA, Ross BD. Diffusion MRI: a new strategy for assessment of cancer therapeutic efficacy. Mol Imaging 2002;1(4):336–343. [PubMed: 12926229]
11. Lee KC, Hall DE, Hoff BA, Moffat BA, Sharma S, Chenevert TL, Meyer CR, Leopold WR, Johnson TD, Mazurchuk RV, Rehemtulla A, Ross BD. Dynamic imaging of emerging resistance during cancer therapy. Cancer Res 2006;66(9):4687–4692. [PubMed: 16651420]
12. Lee KC, Moffat BA, Schott AF, Layman R, Ellingworth S, Juliar R, Khan AP, Helvie MA, Meyer CR, Chenevert TL, Rehemtulla A, Ross BD. Prospective early response imaging biomarker for neoadjuvant breast cancer chemotherapy. Clin Cancer Res 2007;13(2):443–450. [PubMed: 17255264]
13. Lee KC, Sud S, Meyer CR, Moffat BA, Chenevert TL, Rehemtulla A, Pienta KJ, Ross BD. An imaging biomarker of early treatment response in prostate cancer that has metastasized to the bone. Cancer Res 2007;67(8):3524–3528. [PubMed: 17440058]
14. Lee KC, Bradley D, Hussain M, Meyer C, Chenevert T, Jacobson J, Johnson T, Galbán C, Rehemtulla A, Pienta K, Ross B. A feasibility study evaluating the functional diffusion map as a predictive imaging biomarker for detection of treatment response in a patient with metastatic prostate cancer to the bone. Neoplasia 2007;9(12):1003–1011. [PubMed: 18084607]
15. Hamstra DA, Galbán CJ, Meyer CR, Johnson TD, Sundgren PC, Tsien C, Lawrence TS, Junck L, Ross DJ, Rehemtulla A, Ross BD, Chenevert TL. Functional Diffusion Map as an early imaging biomarker for high-grade glioma: Correlation with conventional radiologic response and overall survival. J. Clin Oncol 2008;26(20):3387–3394. [PubMed: 18541899]
16. Ross BD, Chenevert TL, Kim B, Ben-Joseph O. Magnetic resonance imaging and spectroscopy: Application to experimental neurooncology. Q. Magn. Reson. Biol. Med 1994;1:89–106.
17. Meyer CR, Boes JL, Kim B, Bland PH, Zasadny KR, Kison PV, Koral K, Frey KA, Wahl RL. Demonstration of accuracy and clinical versatility of mutual information for automatic multimodality image fusion using affine and thin-plate spline warped geometric deformations. Medical Image Analysis 1997;1:195–206. [PubMed: 9873906]
18. Pickles MD, Gibbs P, Lowry M, Turnbull LW. Diffusion changes precede size reduction in neoadjuvant treatment of breast cancer. Magnetic Resonance Imaging 2006;24(7):843–847. [PubMed: 16916701]

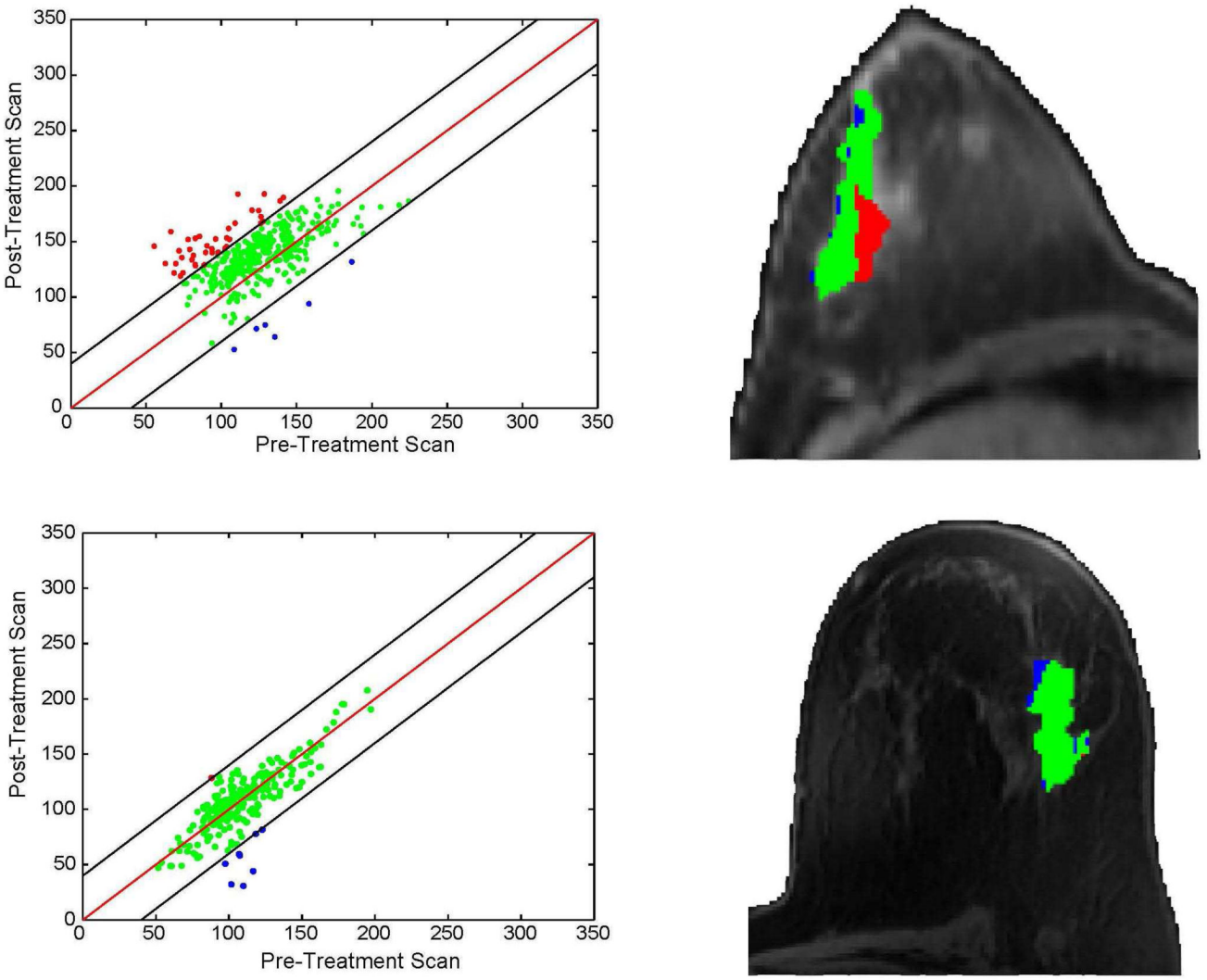

Fig. 1.

Functional diffusion maps for responsive and non-responsive breast treatment. Top and bottom rows respectively show from left to right the treatment effect, and fDM treatment overlay on one anatomical slice. Patient on the top was found to be ER+ while the bottom patient was ER −.

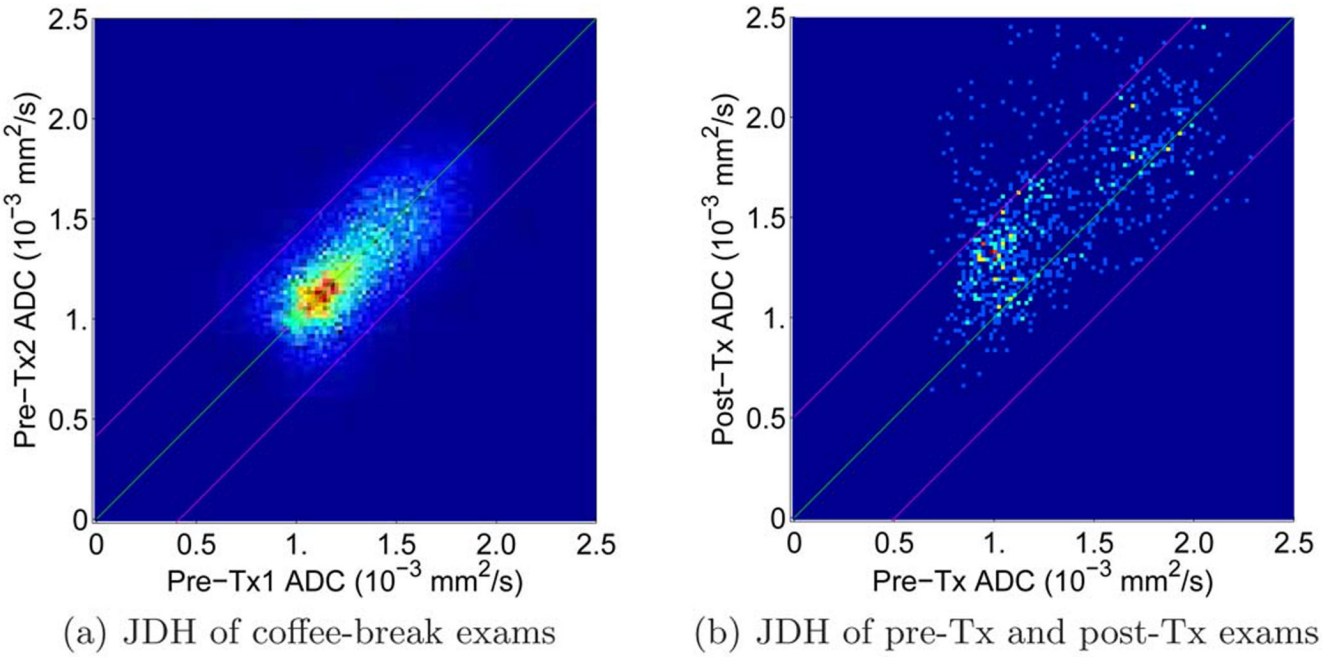

(a) JDH of coffee-break exams (b) JDH of pre-Tx and post-Tx exams

Fig. 2.

Joint distribution histograms. (a) JDH of a pair of pre-treatment coffee-break exams. The green line represents the linear regression of the JDH, which is the diagonal line in this case. The magenta lines represent the 97.5th and 2.5th percentile, respectively; i.e., the area between the magenta lines is 95% confidence interval for the null distribution. (b) JDH of a pair of pre- and post-treatment exams. The green line represents the diagonal line and the magenta lines represent the 97.5th and 2.5th percentile lines of the null distribution, respectively. Note that the magenta lines in (a) and (b) are of different intercepts. The magenta lines in (a) are the 97.5th and 2.5th percentile for this specific coffee-break exam pair. The magenta lines in (b) are the average 97.5th and 2.5th percentile for the 5 pairs of coffee-break exams in the training data sets.

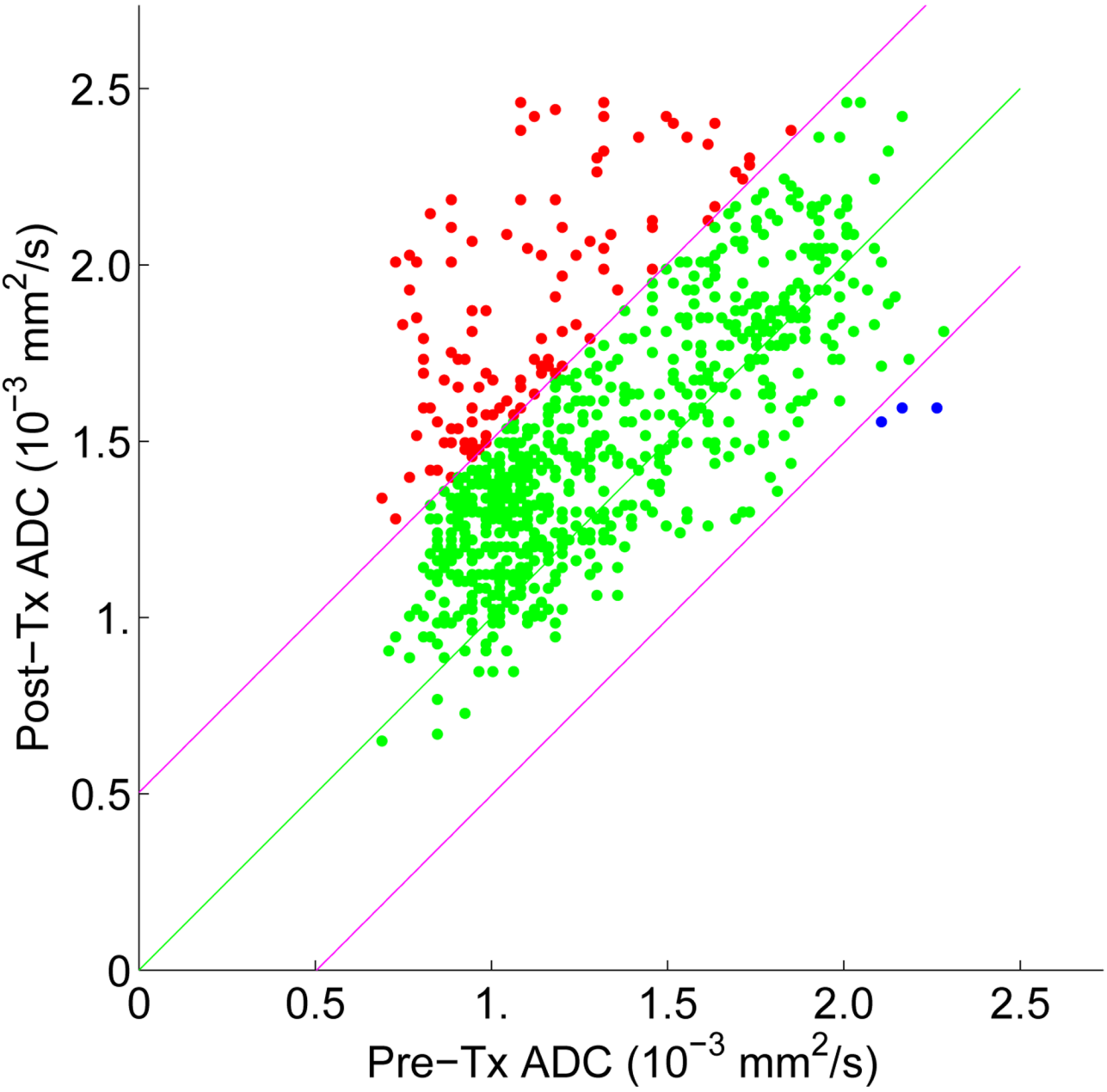

Fig. 3.
fDM analysis in assessing treatment response based on registered diffusion scans obtained shortly after and before the initiation of neoadjuvant therapy for a patient.

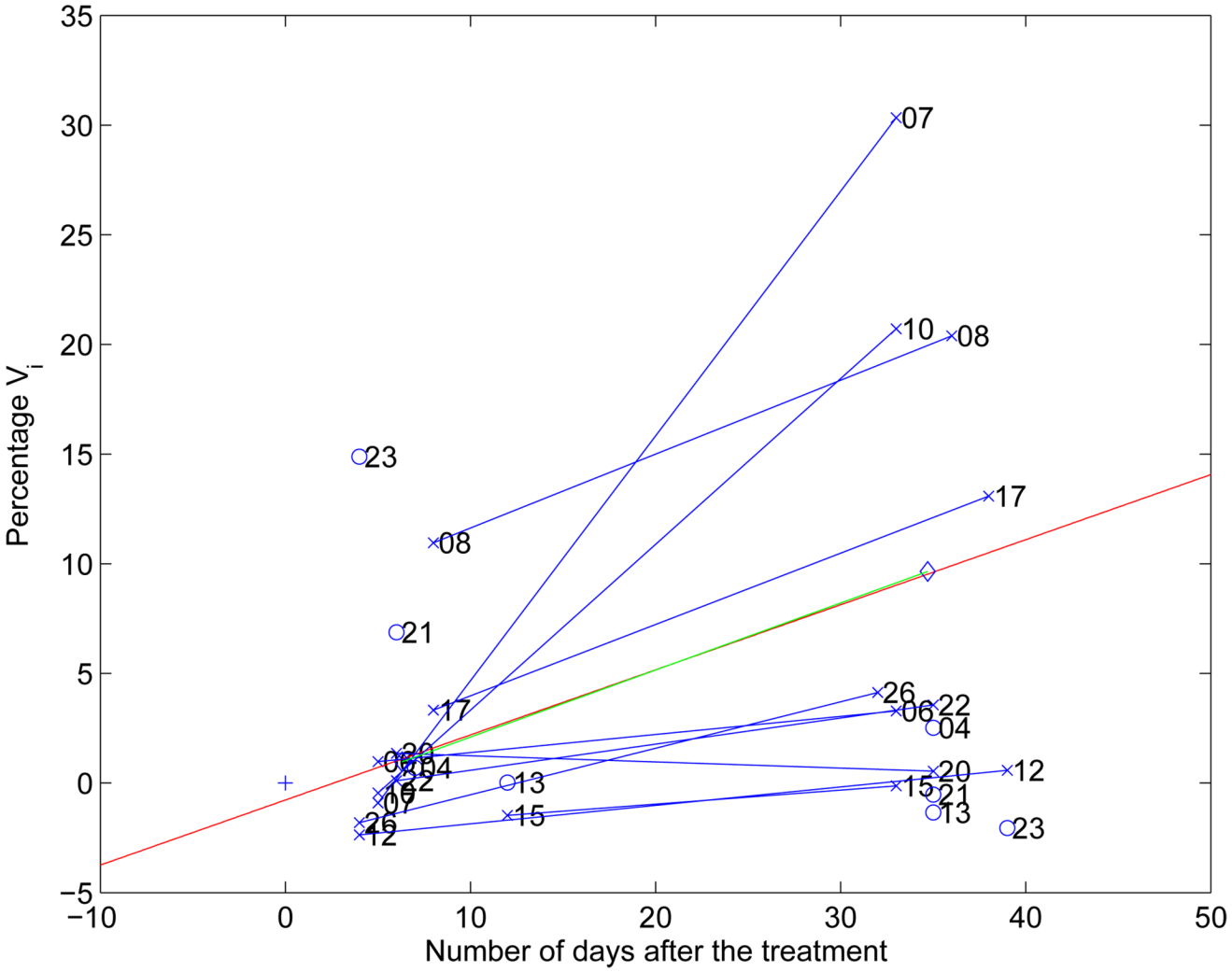

Fig. 4.

Percentage_V_i versus number of days after the initiation of treatment. The red line represents linear regression of all (percentage_V_i, number of days after treatment) pairs. A blue line connects the two different time points for each patient. The (0, 0) point is plotted with a ”+”; Ideally after a zero length time interval there should be no measured response to therapy.